Effect of dopant density on contact potential difference across n-type GaAs homojunctions using Kelvin Probe Force Microscopy

C. Kameni Boumenou[*], Z.N. Urgessa[*], S.R. Tankio Djiokap[*], J.R. Botha[*], J. Nel[**]

[*]Department of Physics, P.O Box 77000, Nelson Mandela Metropolitan University, Port Elizabeth 6031, South Africa
[**]Department of Physics, University of Pretoria, Private bag X20, Hatfield 0028, South Africa
Corresponding author-email address: Christian.kameniboumenou@nmmu.ac.za

Abstract
In this study, cross-sectional surface potential imaging of *n+/*semi-insulating GaAs junctions is investigated by using amplitude mode kelvin probe force microscopy. The measurements have shown two different potential profiles, related to the difference in surface potential between the semi-insulating (SI) substrate and the epilayers. It is shown that the contact potential difference (CPD) between the tip and the sample is higher on the semi-insulating substrate side than on the *n-type* epilayer side. This change in CPD across the interface has been explained by means of energy band diagrams indicating the relative Fermi level positions. In addition, it has also been found that the CPD values across the interface are much smaller than the calculated values (on average about 25% of the theoretical values) and increase with the electron density. Therefore, the results presented in study are only in qualitative agreement with the theory.

Keywords: Kelvin probe force microscopy, n+/semi-insulating GaAs junctions, contact potential.

1. Introduction

Potential profiling of semiconductor devices and semiconductor heterostructures on a nanometer scale has long been an important challenge for material and device engineers [1]. Several measurement techniques have been developed for this purpose. Among these, Kelvin Probe Force Microscopy (KPFM) proposed in 1991 by Nonnenmacher *et al.* [2] appears as the most powerful. It extracts simultaneously the 3D topographic information (with resolution of 1 nm in the x-y plane and 0.1 nm in the z direction) [3] as well as the surface electrical properties of materials on the nanometer scale [4]. In principle, KPFM measures the sample surface potential, by minimizing the interaction force between a sharp conducting tip and the sample surface. The measurement is usually carried out in one of two different modes: Frequency Modulation (FM) or Amplitude Modulation (AM) KPFM. In FM-KPFM mode, the electrostatic force gradient is minimized, while in AM-KPFM mode the electrostatic force itself is minimized. In this study, AM-KPFM is used to investigate the contact potential difference (CPD) across the homojunction between semi-insulating GaAs (SI-GaAs) and n^+- *type* GaAs epilayers with different dopant densities. AM mode KPFM performs the measurements by mainly minimizing the amplitude of the electrostatic force (between the tip and sample) shown in equation (1) [5]:

$$F_{ac} = -\frac{\partial C}{\partial z}(V_{dc} - V_{CPD})V_{ac}\sin(w_{ac}t) \qquad (1)$$

In this equation (1), $\frac{\partial C}{\partial z}$ is the capacitance gradient which depends on the tip geometry and the tip-sample distance z [6], V_{dc} is a *dc* applied voltage, V_{CPD} is the CPD across the interface, V_{ac} is the amplitude of the *ac* applied voltage and w_{ac} its frequency. Details of the measurement setup for AM-KPFM can be found elsewhere [7, 8]. In addition, the procedure to extract the CPD across the interface in a cross-sectional sample is also described by T. Muzutani *et al.* in [1]. As reported by R. Darling [7], the electrostatic properties of any junction depend primarily on the positions of the Fermi levels of the two materials that form the metallurgical junction. For the n^+- GaAs: Si epilayers used in this study, the Fermi level is above the conduction band edge. For the SI-GaAs, in which a deep donor (often known by EL2) is used to compensate the shallow acceptors (carbon or C_{As}), the Fermi level has been reported to be locked slightly above the intrinsic level (*i.e.* mid-gap) [7].This indicates that the equilibrium electron concentration (~10^{16} cm^{-3}) [8] in the bulk semi-insulating region is greater than the equilibrium hole concentration (~10^{15} cm^{-3})[8]. As a result, such SI-GaAs can be considered as slightly *n-*

type. Hence, when a junction is formed between an epilayer (n^+ side) and *n-type* SI-GaAs, the excess electrons from the epilayer side diffuse into the SI region, resulting in a monotonic decrease in electron density across the junction (space charge region) [7]. The hole density follows a complementary profile [7]. Since the electron concentration in the bulk of the SI-GaAs is larger than the hole concentration, this means that the two carrier concentration profiles will not cross in the junction area. Thus, the n^+/SI junction does not exhibit a depletion region [7]. The contact potential differences across *n+/*semi-insulating GaAs junctions, which can be theoretically approximated by using the relationship $\left|\emptyset_{S_b} - \emptyset_l\right|$ where $\emptyset_{S_b}$ is the work function of substrate, $\emptyset_l$ that of the epilayer, are given as:

$$V_{CPD_{d_{GaAs}}} = \left|\frac{1}{2}\left(E_g - \Delta E_g\right) + kT\left[ln\left(\frac{n}{N_c}\right) + \frac{1}{\sqrt{8}} * \frac{n}{N_c} - \frac{3}{4} ln\left(\frac{m^*_{h_{GaAs}}}{m^*_{e_{GaAs}}}\right)\right]\right| \quad (2)$$

where, E_g, k, T, N_c, $m^*_{h_{GaAs}}$ and $m^*_{e_{GaAs}}$ are the energy band gap, Boltzmann's constant, absolute temperature, the effective density of states in the conduction band, the effective mass of holes and the effective mass of electrons, respectively. In this equation, the position of the Fermi energy in the substrate is assumed to be mid-gap. Based on the fact that the measurements conducted in this study have been made in air, the comparison between the experimental and theoretical values is qualitative and not quantitative. The term ΔE_gin equation (2) refers to the band gap narrowing of the *n+* layer, which can be given by [9]:

$$\Delta E_g(meV) = A\left(\frac{n}{10^{18}}\right)^{1/3} + B\left(\frac{n}{10^{18}}\right)^{1/4} + C\left(\frac{n}{10^{18}}\right)^{1/2} \quad (3)$$

In equation (3) A, B and C are constants and have the values 16.30 *meV*, 7.47 *meV* and 90.65 *meV*, respectively [9]. The main goal of this study is to experimentally determine the **built-in potentials** across various *n+/*semi-insulating GaAs homojunction samples using KPFM and to compare these values with the CPD-values given by equation (2).

2 Experimental

This manuscript presents studies carried out on *Si*-doped (*n-type)* degenerate GaAs grown on semi-insulating GaAs (*n*-GaAs/SI-GaAs), using AM-KPFM in air and at room temperature. A Bruker Dimension FastScan scanning probe microscope was used. Four samples with electron densities (as determined by Hall measurements at room temperature) of $\sim(4.9 \pm 1.0) \times 10^{18}\ cm^{-3}$, $\sim(6.3 \pm 1.2) \times 10^{18}\ cm^{-3}$, $\sim(6.5 \pm 1.3) \times 10^{18}\ cm^{-3}$ and $\sim(6.7 \pm 1.4) \times 10^{18}\ cm^{-3}$ have been considered for investigation. The uncertainties in these values represent a maximum estimated error in the Hall concentration of 20%. The samples were grown by metalorganic chemical vapour deposition at a temperature of $\sim$ 740 °C and a V/III growth of $\sim$20. Details of the growth system have been presented elsewhere [10]. The samples were manually cleaved from the back side (using a diamond tip scriber), mounted on a cross-sectional sample holder and investigated within the same day to reduce contamination/oxidation. The measurements have been conducted using SCM-PIT probes with the following nominal characteristics: tip radius $\sim 20nm$, length $200 - 250\mu m$, width $23 - 33\mu m$ and thickness $2.5 - 3.5\mu m$. In addition, a lift height in the range of $50 - 75\ nm$ has been used.

3 Results and discussions

Figure 1 presents cross-sectional (a) topography and (b) potential images of 3 μm thick *n*-GaAs/SI-GaAs. The two images were taken at different regions along the interface between the layer and the substrate. The red curves on the topography and potential images, respectively, are the average scan lines, which indicate the average height and potential across the layer and substrate. The scan size was $6\ \mu m \times 6\ \mu m$. As can be seen from both topography images, the interface across the homojunction is fairly smooth. However, the images show different features. It is also important to note that when different spots were scanned along the freshly cleaved interface, the topography features were always different for each scan area. Hence, it is believed that the features seen in the topography image on the right are due to

contamination resulting from cleaving or sample handling. Similar potential profiles have been obtained for almost every scan region, however. As can be seen from Figure 1, both potential images illustrate two main regions related to the difference in electron density between the substrate and layer. There is no correlation between the topography and potential, indicating that the choice of scan parameters yielded no cross-talk between topography and potential values.

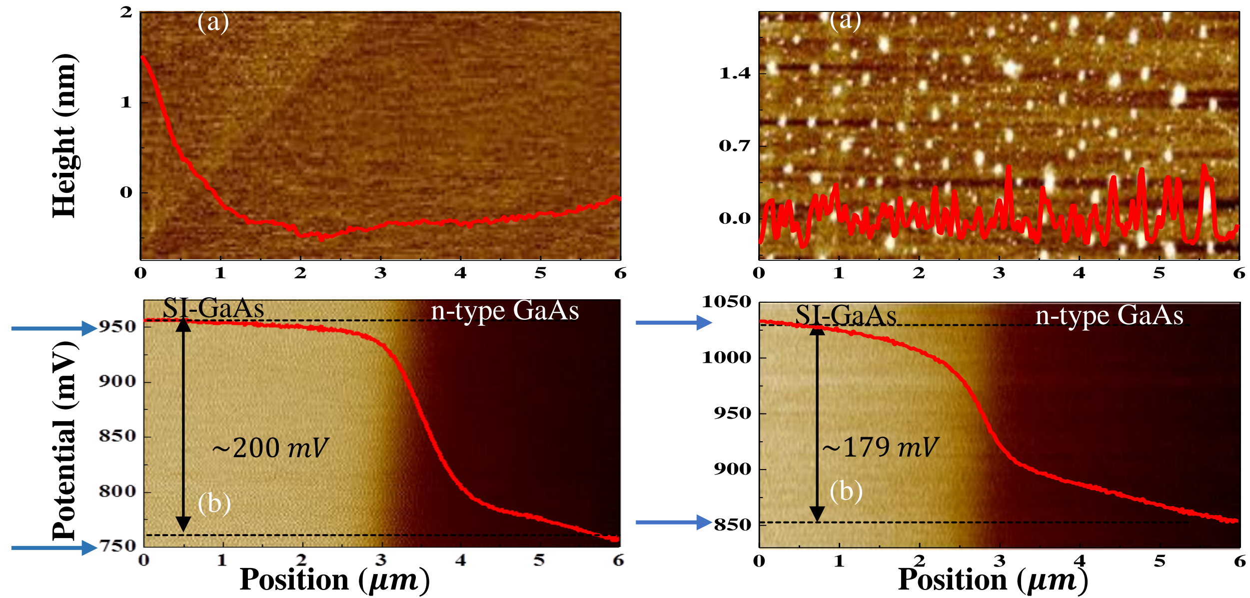

Figure 1: Cross-sectional (a) topography and (b) potential images of 3 μm thick *n-type* degenerate GaAs on SI-GaAs substrate, using AM-KPFM. The two images were taken at different regions along the interface of the same sample. The red curves on the topography and potential images, respectively, are the average height and potential across the two different layers. The scan size was 6 $\mu m \times 6$ μm.

Nevertheless, a broad potential transition is observed. This is related to the limited lateral resolution of AM-KPFM, which is strongly influenced by the size of the tip and the nature of the interaction between the tip and sample. This problem is resolved by measuring the CPD using frequency modulated KPFM, which will be combined with AM-KPFM in a subsequent paper. Furthermore, the values of the CPD of the two spots are slightly different. As shown by the blue arrows on the left-hand side of the potential images, a *dc* voltage of ~950 mV was applied during the KPFM measurements when the tip was on the side of the SI substrate, while a voltage of ~750 mV was applied when the tip was scanning the layer; this gives a CPD of ~200 mV. This value is $\sim$179 mV for the second region. To understand this variation in CPD of the two different regions, the potential profile of a single area was measured by engaging and withdrawing the tip several times. A similar potential profile was observed for the first two scans. However, as the number of engagements and withdrawals increased the value of the *dc* voltage reduced on both side, obviously causing changes in the CPD. This is attributed to the deterioration of the tip or to the automatic adjustment of the amplitude setpoint after the tip engages the sample. The values of the *dc* voltage on the substrate side varied from 1100 mV for the first engagement to 1083 mV for the fourth engagement. For the same scan lines on the layer side, the *dc* voltage varied from ~ 876 mV to ~ 843 mV. Therefore, the error propagation in the CPD between the two sides of the junction is found to be $\sim$ 9 mV. Figure 2 presents cross-sectional potential and topography profiles for four samples with different electron densities. While the topography features vary from sample to sample, the potential profiles of all four samples look similar and there is no correlation between the potential and topography. However, the CPD varies with dopant density. As indicated by the vertical arrows on each potential versus position graph, the value of the CPD for each sample is calculated by taking the difference in potential value on the substrate side and the layer side. To better visualize these variations, the average potential scan lines

of the four samples have been re-plotted on a single graph as shown in Figure 3 (a). For better comparison, the CPD between the tip and substrate has been adjusted to the same value.

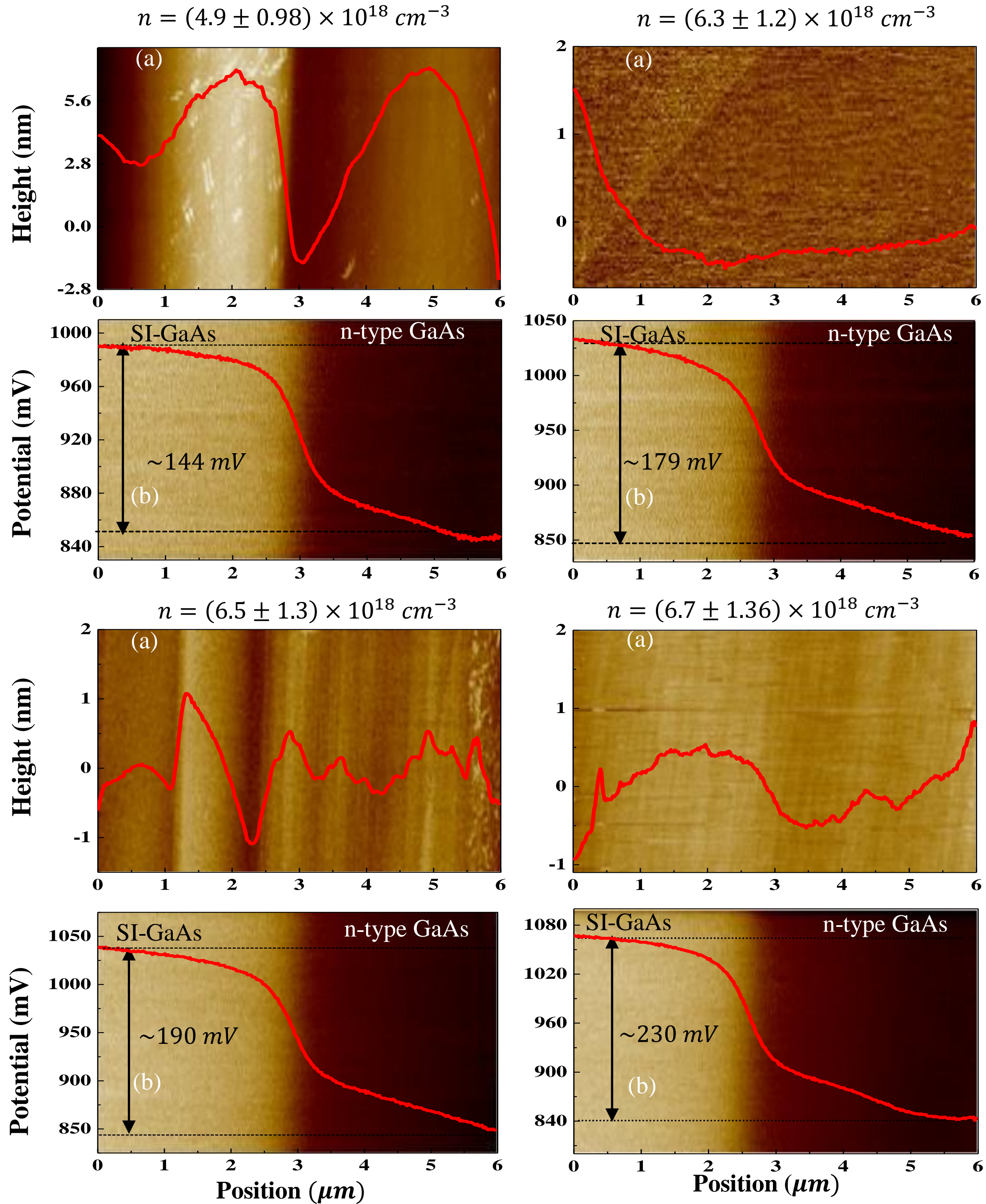

Figure 2: Cross-sectional (a) topography and (b) potential maps of **3 μm** thick *n-type* degenerate GaAs grown on SI-GaAs substrate, using AM-KPFM. Four samples with the same layer thickness, but with different electron densities have been investigated. The red curves on the topography and potential images are the average scans lines, which indicate the shape of the topography and potential across the two different layers. The scan size was **6 μm** × **6 μm**.

As can be seen from Figure 3 (a), the variation in *dc* voltage applied to compensate the CPD between the tip and the layer is significant. This is attributed to the difference in dopant density in the layers. To better illustrate this, the variation of the CPD across the interface has been plotted versus electron density in Figure 3 (b). As mentioned above, the value of the electron density of each sample was obtained using Hall measurements. Regarding the CPD for each sample, the values are obtained from the average potential line scans shown in Figure 2.

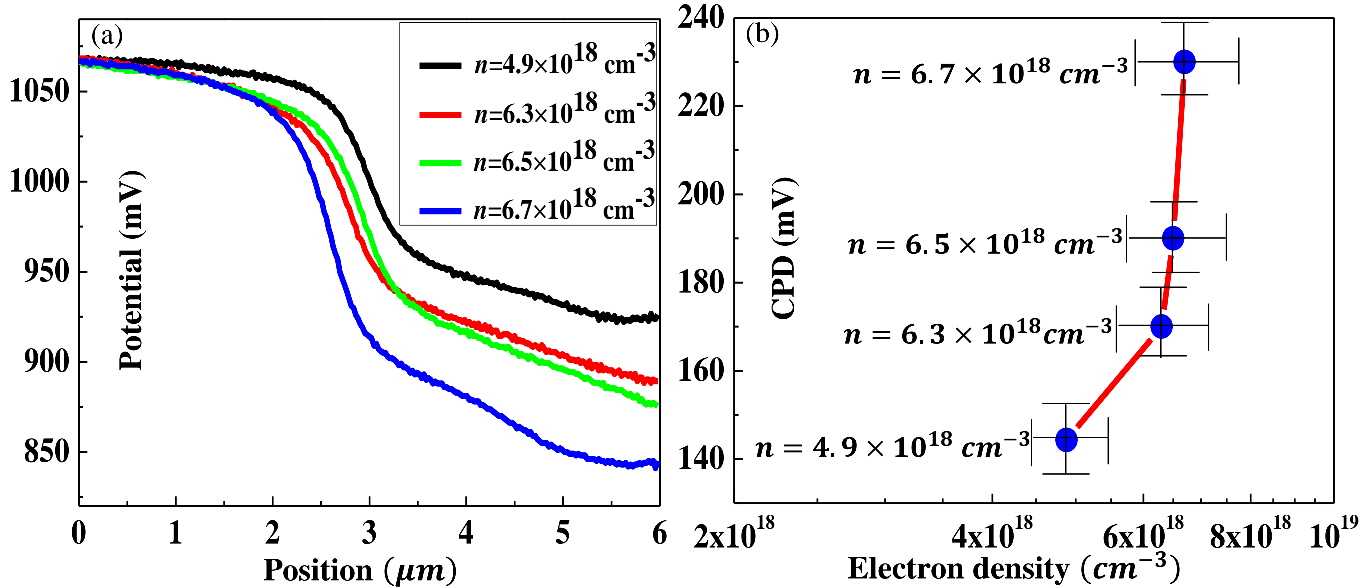

Figure 3: (a) average potential simultaneously plotted of four samples versus position; (b) experimental evolution of the CPD across *n-type* GaAs/ SI-GaAs versus electron density, using AM-KPFM. Vertical and horizontal lines are the estimated CPD and electron density uncertainties, respectively.

As can be seen from Figure 3 (b) the CPD increases by approximately 90 mV as the electron density increases, which is significant given the estimated uncertainty ($\pm 9\ mV$) in each value plotted here. In principle, for an ideal GaAs homojunction, the CDP is equal to the Fermi energy level difference between the substrate and the epilayer. Therefore, the change in potential across the interface can be explained by means of the energy band diagrams shown in Figure 4 [11].

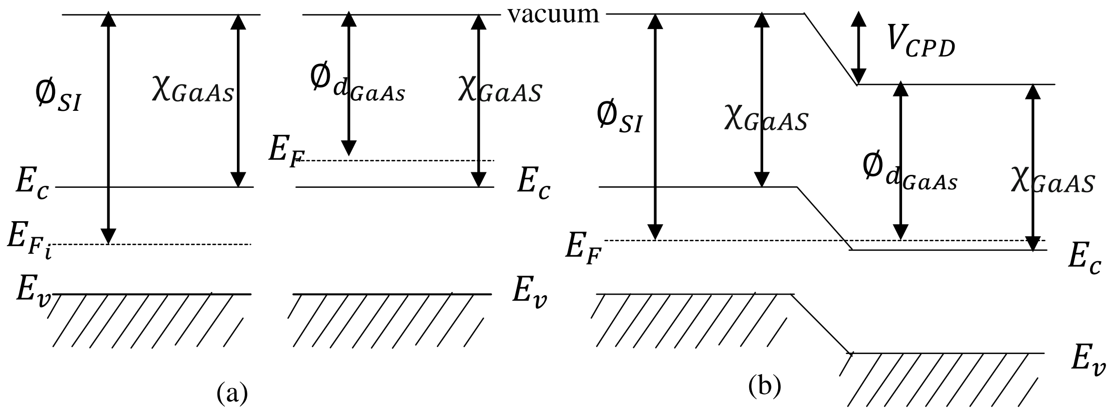

Figure 4: Schematic energy band diagrams for ideal semi-insulating and *n-type* GaAs. (a) Before contact, (b) after contact. $\emptyset_{d_{GaAs}}$, ***and*** $\emptyset_{SI}$ are the work functions of *n-type* degenerate GaAs and SI-GaAs, respectively; $\boldsymbol{E_{F_i}}$ and $\boldsymbol{E_F}$ are the intrinsic Fermi level energy and the Fermi level of *n-type* degenerate GaAs; $\boldsymbol{E_c}$ and $\boldsymbol{E_v}$ are the absolute minimum of the conduction band and absolute maximum of the valence band and $\boldsymbol{\chi_{GaAs}}$ is the electron affinity.

Before contact, the two semiconductor materials are neutral throughout. After contact, because of the difference in work function, charge flows from the semiconductor with the higher Fermi level to the semiconductor with the lower one until the Fermi levels are aligned. This results in a built-in-potential (CPD) between the two layers and non-neutral space charge region on both sides of the interface. To reflect these changes, there is a drop in local vacuum level across the interface (Figure 4 (b)) [11]. This band alignment also illustrates the change in potential across the interface between the two layers ($V_{CPD,}$ Figure 4 (b)). Hence, one would expect that the CPD across the interface is approximately equal to the Fermi energy or work function difference between semi-insulating GaAs and *n-type* GaAs. As indicated earlier, the Fermi level of SI-GaAs was assumed to be pinned approximately at the intrinsic level. On the $n+$ side it is known that as the dopant density increases, the position of the Fermi level also increases [7]. Therefore, the lower the Fermi energy position of the *n-type* film is (for example, for a sample with a lower electron density), the smaller will be the CPD between it and the substrate, as observed in Figure 3 (b). It is important to note that for similar homojunction samples with dopant densities below $\sim(1 \pm 0.2) \times 10^{17} cm^{-3}$, a flat potential across the interface was obtained. This is ascribed to the fact that the two Fermi levels (*i.e.* for the substrate and the layer) are too close to each other for the system to detect, under ambient conditions, any difference between them. Based on the fact that KPFM measurement in air is strongly affected by the ambient, this hypothesis needs to be further investigated by measurements in vacuum, where absolute values of the CPD can be measured [5].
It should be mentioned that there are significant differences in the values of the theoretically predicted and experimentally observed CPD values. Theoretically, the CPD versus dopant density can be simulated by using equation (2). The calculated CPD values versus dopant density (n) are shown in Figure 5. For GaAs at room temperature, $E_g = 1.424$ eV , $N_C = 4.7 \times 10^{17}\ cm^{-3}$, $\frac{m^*_{h_{GaAs}}}{m^*_{e_{GaAs}}} = 7.07$. The dopant density dependent ΔE_g has been included.

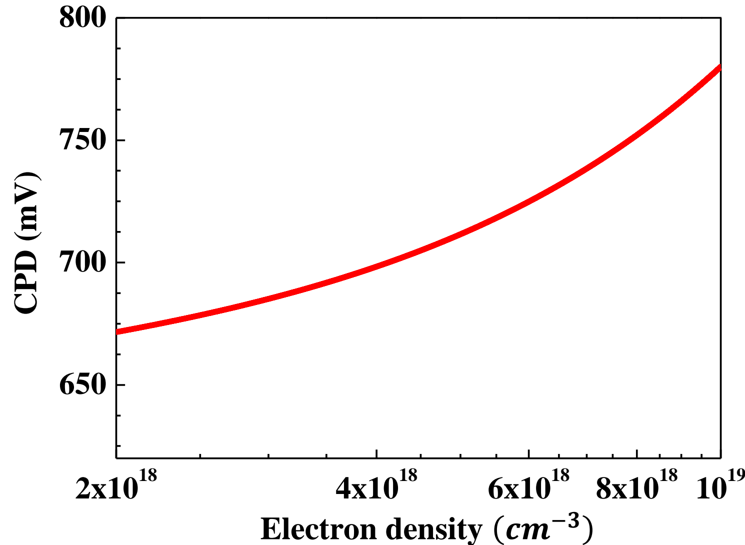

Figure 5: Theoretical evolution of the CPD across the *n-type* GaAs/SI-GaAs interface versus electron density.

As pointed out above, the experimental CPD values are much smaller than the calculated values (on average about 25% of the theoretical values). This discrepancy can be attributed to surface traps due to the exposure of the sample to air and to incomplete ionization of the donor atoms in a degenerately doped layer, as pointed out by F. Robin *et al.* in [12], where they observed that the built-in-potential measured in air across a cleaved p-i-n laser diode, was around 40% of the simulated values. In addition, this

discrepancy can also be explained by the shape of SCM-PIT cantilever used to perform the current AM-mode measurements. Due to its large length, width and tip radius, the CPD values measured are not truly local but rather a convolution over the large area covered by the cantilever. This means that when the tip is scanning across the junction, the potential measured is probably a convolution of that of the substrate and that of the layer.

4 Conclusion

In conclusion, the built-in potential across *n+/*semi-insulating GaAs junctions have been investigated. The potential profiles obtained contain two main regions, related to the difference in electron density between the SI-substrate and the epilayer. The study indicated that the CPD between the tip and the semi-insulating substrate is higher than that of the CPD between the tip and the *n-type* epilayer, which implies that the Fermi level of the epilayer is higher than that of the semi-insulating side. This change in CPD across the interface has been explained by considering the Fermi energy alignment across the interface. In addition, it has also been found that the magnitude of the CPD is much smaller than the calculated values (on average about 25% of the theoretical values) and that increases with the electron density. Therefore, the results presented in study is only qualitative.

Acknowledgments

This work is based upon research supported by the SA Research Chairs Initiative of the Department of Science and Technology and the National Research Foundation. The financial support of the Nelson Mandela Metropolitan University is also gratefully acknowledged.

References

[1] T. Muzutani, T. Usunami, S. Kishimoto and K. Maezawa, *Jpn. J. Appl. Phys.,* vol. 37, p. 767, 1999.

[2] M. Nonnemacher, M. P. O'Boyle and H. K. Wickramasingle, *Appl. Phys. Lett.,* vol. 58, p. 2921, 1991.

[3] R. Bozek, *Acta Phys. Pol., A.,* vol. 108, p. 541, 2005.

[4] W. Melitz, J. Shen, A. Kummel and S. Lee, *Surf. Sci. Rep.,* vol. 66, p. 1, 2011.

[5] T. Glatzel, S. Sadewasser, and M. C.Lux - Steiner, *Appl. Surf. Sci.,* vol. 210, p. 84, 2003.

[6] U. Zerweck, C. Loppacher, T. Otto, S. Grafström and M. Lukas, *Phys. Rev. B,* vol. 71, p. 125424, 2005.

[7] R. B. Darling, *J. Appl. Phys.,* vol. 74, p. 4571, 1993.

[8] D. S. Mcgregor, R. A Rojeski, G. F.Knoll, F. L. Terry, Jr, J. East and Y. Eisen, *Nucl. Instr. and Meth. in Phys Res . A,* vol. 343, p. 527, 1993.

[9] S. C. Jain and D. J. Roulston, *Solid-State Electronics,* vol. 34, p. 453, 1991.

[10] H. L. Ehlers, A. W. R. Leitch and J. S. Vermaak, *J. Cryst. Growth,* vol. 96, p. 101, 1989.

[11] T. Glatzel, S. Sadewasser and M. C.Lux - Steiner, *Mater. Sci. Eng., B,* vol. 102, p. 138, 2003.

[12] F. Robin, H. Jacobs, O. Homan, A. Stemmer and W. Bachtold, *Appl. Phys. Lett.,* vol. 76, p. 2907, 2000.